Flare Analysis for Multiple Stellar Cluster Data from ANCHORS Database.

N. Bizunok (CfA), M. Bruck (Willians College), S. J. Wolk, B. Spitzbart, N. R. Evans (CfA), and J. M. Pasachoff (Williams College)

Abstract:

We present a progress report on a study of flares in young stellar clusters. We use 19 clusters from ANCHORS (An Archive of Chandra Observations of Regions of Star Formation) database and flare criteria derived previously from COUP (Chandra Orion Ultradeep Project). Most of the clusters have ages between 0.05 and 4 Myr and exhibit flaring behavior between 0 and 0.5 flares/day.

Motivation: Stellar flares are strong disturbances in magnetic field structure in stellar atmospheres that result in violent outbursts of plasma and radiation. Identifying stars and young stellar objects that flare and studying their properties aids in understanding stellar magnetic field structures as well as evolution of proto planetary disks and stellar environments. While COUP presents a large catalog of stars with extensive variability sampling from the Orion Cloud region, ANCHORS data offers a complementary sample from a variety of environments. As a part of our ANCHORS database creation, we subject our sources' light curves to Bayesian Blocks analysis, which allows us to search for flaring behavior.

Magnetic Activity in Young Stars

Young stellar objects or YSO's (Age<10 million years) exhibit very high levels of magnetic activity, causing x-ray flare events. Past studies have indicated magnetic fields of 1000-3000 gauss covering the surfaces of these stars, while photometric and Doppler imaging reveal that, like our Sun, these fields are complex and highly variable. YSO theoretical flare models are based upon solar-type cylindrical magnetic field tubes (Feigelson & Montmerle 1999).

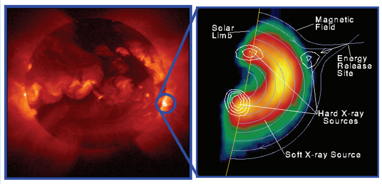

Yohkoh X-ray Image of a Solar Flare, Combined Image in Soft X-rays (left) and Soft X-rays with Hard X-ray Contours (right). Jan 13, 1992.

ANCHORS Flares: Bayesian Blocks Statistics

We use Bayesian Blocks analysis to subdivide X-ray light curves into maximum likelihood blocks as a part of our standard processing routine for each cluster we work with. Bayesian Blocks analysis was devised by Jeffery Scargle in 1998 and implemented as a package of S-Lang scripts, which we use for our data. Bayesian Blocks analysis uses maximum likelihood Bayesian Statistics in order to optimally subdivide light curves into segments of equivalent count rate and allow the data itself to determine the timescale on which photon rate variability can be found. Below is an example of Bayesian Blocks analysis performed on a X-ray point source in OMC 2-3:

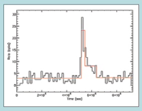

The source on the left is a part of ANCHORS Database. The black line indicates the X-ray light curve, and the red line shows a Bayesian Blocks fit. The result of such a fit allows for global ANCHORS database searches for X-ray flares for all detected point sources with sufficient count statistics.

(See *http://space.mit.edu/CXC/analysis/SITAR/* for J. Scargle's paper on Bayesian Blocks)

COUP Flare Study and Mathematical Flare Definition:

From 9.7 days of effective exposure of the Orion Nebula Cluster, the COUP team has derived empirical constraints to quantify the length of a flaring structure. Wolk et al. (2005, ApJS, 160, 423) have selected criteria for flare identification from 41 flares in COUP data. Partitioning of the light curves in a maximum likelihood algorithm, similar to Bayesian Block method by Scargle (see above), they searched for the periods of constant brightness and identified the points at which there was a significant change, thus separating the curves into *Maximum Likelihood Blocks* (MLBs). These blocks represented the behavior of photon count rate as they arrived to the detectors from each source. In order to differentiate stochastic behavior (random low-sigma fluctuations) from an abrupt change in brightness (orders of magnitude change indicating a flare), a *characteristic "quiescent" count rate*, R_{char}, was defined by maximizing the number of blocks that fell within the range $0.5R_{block}-1.5\sigma \le R_{char} \le 1.2R_{block}+1.5\sigma$, where R_{block} is the count rate of each block and σ is its significance. Slopes between consecutive blocks were defined as dR/dt, where dR was the change in count rate and dt was the lengh of the shorter block. A flare was then defined as a region on which at least one MLB had $(1/R_{characteristic\ rate})*(dR/dt) > 10^{-4}\ sec^{-1}$

ANCHORS Flare Analysis Guidelines:

- $(Block_i) > 1.2*(Block_{characteristic\ rate}) + 2.5*(Error_{Block characteristic\ rate})$ and
- $(1/R_{characteristic\ rate})*(dR_{Block\ i}/dt) > 10^{-4}\ sec^{-1}$ identify a flare.

The first condition says that a Bayesian Block that indicates a flare should be higher than the characteristic rate (longest quiescent level block) as shown. The second condition states that the normalized rate of change from the quiescent level to a flare level should be greater than the order of 10^{-4}. *dt* is the duration of Bayesian Block$_i$.

- Only blocks of greater than 1ks duration were considered significant for flare identification.
- First and last blocks were accounted for by setting the lower limit on their duration to 2ks.

Brief Description of ANCHORS Database as a Sample Page Output:

- *Top images (1 sq. acrsec FoV)*: 2MASS J, H, and K combined field (left) and Chandra observation (right)
- *Spectral Fits* (below figures): Each spectrum with sufficient counts was fitted in a variety of ways. For a relatively strong spectrum, both a single temperature and two temperature Raymond-Smith models were fitted (top and bottom rows respectively.) Fitting parameters are the column density (WABS), the temperature, the absorbed flux, the unabsorbed flux, and the reduced χ^2. Plots of the fits are shown below the table, with the residuals under the spectrum.
- In addition to the spectral fits (bottom), quantile analysis, Bayesian block variability analysis, and 2MASS data are provided. Quantile analysis determines the energy below which a fraction of the counts are found (e.g. 25% of the counts in table are found below 1.203 keV). The Bayesian block analysis (table and the figure) divides the light curve into intervals with different flux levels.

(For information on ANCHORS, please refer to B. Spitzbart's poster)

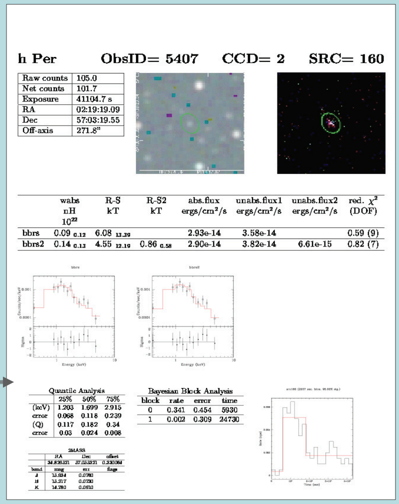

Flares, Variability in 19 ANCHORS Clusters/Observations:

Cluster Name	# Sources (tot. detected)	# Sources	% >1 block	% with Flares	Error for % w. Flares	Exp. Time (ksec)	Age (Myr)	Flare Rate (flares/day)
		(all greater than 50 counts)						
h Persei	178	23	26.1	21.7	9.72	40	10-20	0.47
inter h Persei	17	5	40.0	0.0	0.00	10	?	0.00
Pleiades	52	23	17.4	13.0	7.53	21.49	70-100	0.52
NGC 1333	90	37	59.5	13.5	6.04	43.91	<1	0.27
Lynds 1551	68	23	17.4	0.0	0.00	79.94	~0.1	0.00
Cha I North	104	40	27.5	10.0	5.00	67.14	0.3-0.5	0.13
NGC 2024	266	150	36.7	12.7	2.91	76.43	0.3-0.5	0.14
Monoceros R2	370	124	26.6	8.9	2.67	98.08	1-3	0.08
NGC 2264[1]	372	221	31.2	10.4	2.17	96.97	2-4	0.09
NGC 2264[2]	251	135	34.1	3.7	1.66	48.76	2-4	0.07
ONC Flanking. field	221	128	37.5	10.2	2.82	48.46	1-3	0.18
ONC Flanking. field	196	100	30.0	5.0	2.24	49.43	1-3	0.09
Maddalena's Cloud	54	9	0.0	0.0	0.00	29.16	?	0.00
IRAM 04191	26	7	0.0	0.0	0.00	19.16	<0.05	0.00
RCW 49	302	35	17.1	8.6	4.95	36.66	~1	0.20
NGC 1579[3]	146	41	26.8	7.3	4.22	40	~1	0.16
NGC 1579[4]	146	51	29.4	9.8	4.38	40	~1	0.21
OMC 2-3	295	213	46.5	13.1	2.48	89.17	<3	0.13
Serpens core	88	44	34.1	4.5	3.21	88.45	2	0.04
NGC 1333 N[5]	41	23	47.8	17.39	8.70	43.91	<1	0.72
NGC 1333 S[6]	52	14	78.6	7.14	7.14	43.91	<1	0.18

[1,2] NGC 2264 North/South fields, [3,4] NGC 1579: 2 pointings separated by ~1 day, [5,6] NGC 1333: North and South halves of the observed field.

This table shows the results of flare and variability search in 19 different observations. Variable sources (those with more than 1 significant block) are listed in column 4. Flaring sources are listed in column 5. Both are given for each observation as percentages of the total number of sources with greater than 50 counts. Flare rate (last column) is derived from multiplying the number of flaring sources by the inverse of the product of total number of sources (with more than 50 counts) and exposure time.

The last two lines show calculations for north and south halves of the NGC 1333 field because, we believe, there are differences in flare rates between the two regions.

The two plots below correlate the values from the table on the left.

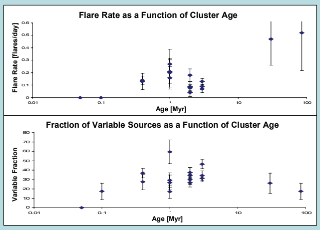

Conclusion: Chandra observations are sensitive to flares and variability from very young clusters. On the plots above, there is a paucity of clusters with ages between ~1-100Myr due to biases in Chandra's target selection. In order to constrain the variability and flaring behavior of stars as a function of cluster age, this gap needs to be filled in. Existing XMM data analysis should help as well as Chandra observations of older clusters.

Below: 1) Example of a flaring source in OMC 2-3. The small table to the left of the plot shows Bayesian Blocks fit in terms of rate, rate error, and duration for each block. 2) Example of a flaring source in NGC 1333.

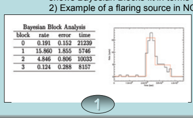

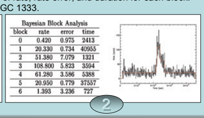

2MASS Colors for Flaring Sources in Select Observations:

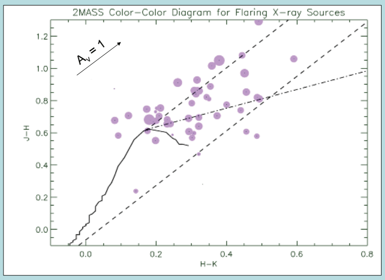

The plot above shows 2MASS colors for h Persei, Pleiades, NGC 1333, ONC Flanking Fields, RCW 49, NGC 1579, OMC 2-3, and Serpens core (70 stars altogether). Purple circles indicate the size of photometric errors. The smaller the circle, the larger the photometric error of its corresponding source is. This representation facilitates identifying sources with more reliable photometry. The slope of the reddening vector is taken from Meyer et al, 1997. Parallel tracks along the direction of reddening are taken from their work as well. The solid black curve indicates the main sequence.

Conclusion: There is no evidence in the data that any of the flaring stars are disk candidates.

Please send your questions and comments to N. Bizunok at nbizunok@cfa.harvard.edu